Fascin1 suppresses RIG-I-like receptor signaling and interferon-β production by associating with IκB kinase ε (IKKε) in colon cancer

Tomio Matsumura[‡§¶], Shigeaki Hida[ǁ], Masato Kitazawa[¶], Chifumi Fujii[‡#], Akira Kobayashi[¶], Michiko Takeoka[¶], Shun-ichiro Taniguchi[‡], and Shin-ichi Miyagawa[¶]

From [‡] Department of Molecular Oncology, [§]Department of Aging Biology, Shinshu University Graduate School of Medicine, [¶]Department of Surgery, Shinshu University School of Medicine, [#]Department of Advanced Medicine for Health Promotion, Institute for Biomedical Sciences, Shinshu University, Matsumoto 390-8621, Japan and [ǁ]Department of Molecular and Cellular Health Science, Nagoya University Graduate School of Pharmaceutical Sciences, Nagoya 467-8603, Japan

Running title: Fascin1 suppresses RIG-I signaling

To whom correspondence should be addressed: Prof. Shin-ichi Miyagawa, Department of Surgery, Shinshu University School of Medicine, Matsumoto 390-8621, Japan. Telephone: 81-263-37-2654; FAX: 81-263-35-1282; E-mail: shinichi@shinshu-u.ac.jp and Prof. Shigeaki Hida, Department of Molecular and Cellular Health Science, Nagoya University Graduate School of Pharmaceutical Sciences, Nagoya 467-8603, Japan. Telephone: 81-; 052-836-3592, FAX: 81-; 052-836-3419, E-mail: hida@phar.nagoya-cu.ac.jp

Keywords: fascin1, poly (I:C), RIG-I-like receptor, interferon regulatory factor-7, interferon-β, IκB Kinase ε, signal transducers and activators of transcription, DLD-1, invasion

---

ABSTRACT

Fascin1 is an actin-bundling protein involved in cancer cell migration and has recently been shown also to have roles in virus-mediated immune cell responses. Because viral infection has been shown to activate immune cells and to induce IFN-β expression in human cancer cells, we evaluated the effects of fascin1 on virus-dependent signaling via the membrane- and actin-associated protein retinoic acid-inducible gene I (RIG-I) in colon cancer cells. We knocked down fascin1 expression with shRNA retrovirally transduced into a DLD-1 colon cancer and L929 fibroblast-like cell lines and used luciferase reporter assays and co-immunoprecipitation to identify fascin1 targets. We found that intracellular poly (I:C) transfection to mimic viral infection enhances the RIG-I/melanoma differentiation-associated gene 5 (MDA5)-mediated dimerization of interferon regulatory factor 3 (IRF-3). The transfection also significantly increased the expression levels of IRF-7, IFN-β, and interferon-inducible cytokine IP-10 in fascin1-deleted cells compared with controls while significantly suppressing cell growth, migration, and invasion. We also found that fascin1 constitutively interacts with IκB Kinase ε (IKKε) in the RIG-I signaling pathway. In summary, we have identified fascin1 as a suppressor of the RIG-I signaling pathway associating with IKKε in DLD-1 colon cancer cells to suppress immune responses to viral infection.

Fascin1 is an evolutionarily conserved 55-kDa actin-bundling protein that is localized in filopodia, which are involved in cell migration, as well as actin-based protrusions beneath the plasma membrane (1,2). Fascin1 protein plays an important role in the regulation of cell adhesion, migration and invasion in breast cancer (3), colon cancer (4), and melanoma (5) and is closely correlated with a poor prognosis and survival in cancer patients.

As the inhibition of fascin1 function leads to a block in tumor metastasis (6,7), it is considered a potential therapeutic target for tumors. On the other hand, fascin1 is also reportedly involved in immune responses, such as cytokine production (8).

The discovery of tumor cells mimicking an innate immunity pathway after viral infection has attracted considerable attention. For example, the activation of RIG-I (retinoic acid-inducible gene 1) and MDA5 (melanoma differentiation-associated gene 5), both of which are viral RNA recognition molecules, in tumor cells can induce immunogenic cell death in melanoma (9) and leukemia cells (10). A synthetic analog of dsRNA, poly (I:C), activated the pathway mediated by MDA5/RIG-I/IRF (interferon (IFN)-regulatory factor)-3 to express immunoadjuvant IFN-β in PC3 and DU145 cell lines derived from a prostate cancer metastasis (11) and in pancreatic cancer cells (12). Regarding colon cancer, dsRNA induced by demethylation activated MDA5 and elicited the downstream activation of interferon promoter stimulator-1 (IPS-1), IRF-7, and type III IFNs and the up-regulation of IFN-responsive genes in a LIM1215 colorectal cancer cell line (13).

RIG-I, which is reportedly localized in membrane ruffles, associates with the actin cytoskeleton in the human colon adenocarcinoma cell line HT-29 (14) and in the immortalized human intestinal cell line Caco-2 (15). The reorganization of the actin cytoskeleton leads to RIG-I relocalization and induces type I IFNs in Caco-2 cells (15). These findings have culminated in the hypothesis that fascin1 is involved in the RIG-I pathway in colon cancer.

We herein investigated the effects of fascin1 on cell growth and invasion in the RIG-I immune pathway by stimulating the DLD-1 colon cancer cell line with poly (I:C). To our knowledge, this is the first report to clarify the role of fascin1 in dsRNA-dependent RIG-I signaling in the promotion of metastasis in cancer cells, a function that is distinct from the protein's known cytoskeletal properties.

RESULTS

Knockdown of fascin1 suppressed cell migration and invasion—To examine the roles of fascin1 in tumor cells, we first stably deleted fascin1 using shRNA in DLD-1 cells and L929 fibroblast-like cells. The expression levels of mRNA and protein in fascin1 shRNA-transfected cells were effectively decreased to 25% and 20% of those in the control cells, respectively, in DLD-1 cells (Fig. 1A). Consistent with a previous report (16), a morphological analysis elucidated that filopodia formation, but not lamellipodia formation, was impaired in fascin1-deleted L929 cells (Fig. 1B), indicating that fascin1 is a specific actin cross-linker that provides stiffness for filopodial bundles. Regarding cell growth, no difference was observed between DLD-1 cells with or without fascin1 (Fig. 1C), whereas the knockdown of fascin1 suppressed DLD-1 cell migration and invasion (Fig. 1D). These findings showed that fascin1 promoted cell motility in DLD-1 cells. Fascin1-mediated filopodia assembly has been reported to be dispensable for mouse development, and fascin1-deficient mice are viable and fertile with no major developmental defects (17).

Knockdown of fascin1 enhanced RIG-I/MDA5-mediated IRF-7 and IFN-β induction by poly (I:C) transfection—We focused on two receptors for viral RNA, TLR3 (Toll-like receptor 3) and RIG-I-like receptors. IFN-β mRNA production was similar in DLD-1 cells with or without fascin1 when poly (I:C) was applied extracellularly (Fig. 2A), implying no involvement of fascin1 in the TLR3 pathway. The expression of TLR3 in DLD-1 cells has been confirmed by Sadik et al. (18), and we also have data showing the expression of mRNA (data not shown). Although the dose of poly (I:C) was increased from 5 μg/mL (equivalent to the intracellular dose) to 30 μg/mL, extracellularly administered poly (I:C) did not cause IFN-ß mRNA expression to differ between control cells and fascin1-deleted cells. This result was supported by another poly (I:C) performed at a dose of 5 μg/mL to 100 μg/mL (data not shown).

When poly (I:C) was transfected

intracellularly, however, the expression levels of IFN-β and IP-10 (interferon-γ-inducible protein-10) mRNA were significantly increased in fascin1-deleted DLD-1 cells, with no difference observed without poly (I:C) treatment. These results were supported by L929 cell assays (Fig. 2B). Furthermore, the mRNA expression levels of RIG-I, MDA5, IRF-7, and IFN-stimulated genes including IFN-induced protein with tetratricopeptide repeats (IFIT) 1, 2, and 3 were increased by poly (I:C) transfection in fascin1-depleted DLD-1 cells (Fig. 2C), indicating that fascin1 suppressed IRF-7 and IFN-β expression levels via the RIG-I/MDA5-dependent signaling pathway by poly (I:C) stimulation. To confirm the suppressive effect of fascin1 on IFN-ß mRNA expression, we conducted a rescue experiment by the re-expression of fascin1 in fascin1-deleted DLD-1 cells treated with poly (I:C). The increase in IFN-ß mRNA expression arising from fascin1 knockdown was significantly suppressed by the re-expression of fascin1 (Fig. 2D).

Knockdown of fascin1 enhanced IRF-3 activation—Since transcription of the IFN-β gene requires the activation of IRF-3, NF-κB, and several other transcription factors (19), we assessed whether fascin1 contributed to the activation of IRF-3 or NF-κB/p65. As shown in Figure 3A, a poly (I:C) time-dependent definite increase in IRF-3 phosphorylation was detected in fascin1-deleted DLD-1 cells, compared with control cells, using an immunoblot analysis. The dimerization of IRF-3 at 6 h after poly (I:C) transfection supported this result (Fig. 3B). The phosphorylation of the NF-κB subunit p65/RelA was examined next. The amount of phosphorylated p65/RelA protein increased in a time-dependent manner in response to poly (I:C) transfection; however, the levels were comparable between fascin1-deleted cells and controls (Fig. 3C). These data suggest that fascin1 suppresses the activation of IRF-3, but not the activation of the NF-κB signaling pathway.

Fascin1 constitutively associated with IKKε in RIG-I signaling—The knockdown of fascin1 was found to enhance IRF-3 activation and the production of IRF-7, IFN-β and IFITs via the RIG-I/MDA5 signaling pathway (Fig. 2B, 2C). Therefore, we conducted IFN-β luciferase reporter assays to further investigate the molecules affected by fascin1. Fascin1 dose-dependently inhibited IFN-β luciferase reporter activity induced by the overexpression of RIG-I, IPS-1, TBK1 (TANK-binding kinase-1) and IKKε, but not that by IRF-3(5D) (Fig. 4A). The inhibition of IKKε-induced IFN-β by fascin1 overexpression was slight but dose-dependent, indicating an association between fascin1 and IKKε. Together with IRF-3, which did not alter IFN-β production, fascin1 was considered to abrogate IFN-β production by interfering with the function of IKKε. To confirm that fascin1 interacted with IKKε, we next performed co-immunoprecipitation experiments with combinations of vector plasmids expressing Myc-tagged fascin1 (pcDNA3) and FLAG-tagged TBK1, IKKε or IRF-3 (pFLAG-CMV4). As expected, IKKε and IRF-3, but not TBK1, co-immunoprecipitated with fascin1 (Fig. 4B). To verify these results, we conducted reciprocal co-immunoprecipitation assays. As shown in Fig. 4C, fascin1 co-precipitated with IKKε, but not with TBK1 or IRF-3. Thus, fascin1 was confirmed to constitutively interact with IKKε, rather than with RIG-I, IPS-1, TBK1 or IRF-3.

Human IKKε contains a kinase domain (KD), an ubiquitin-like domain (ULD), a leucine zipper (LZ) and helix-loop-helix (HLH) region (20). To better characterize fascin1/IKKε interactions, deletion mutants of these domains were engineered and co-immunoprecipitation analyses were performed. Fascin1 only associated with deletion mutants containing the KD region (Fig. 4D). Fascin1 is also well known to bind F-actin and PKC-α. To evaluate whether F-actin or PKC-α binding sites of fascin1 were essential for IKKε associations, we constructed fascin1 S39A (PKC-α binding site), fascin1 H392A, and fascin1 A488W (F-actin binding site) mutants for co-immunoprecipitation assays with IKKε. IKKε associated with all of these mutants (Fig.

4E), indicating that the kinase domain of IKKε was required for binding to fascin1 in a manner independent of the protein's F-actin or PKC-α binding domains. These three fascin1 mutants inhibited IFN-β luciferase reporter activity induced by the overexpression of RIG-I, similar to the actions of wild-type fascin1 shown in Figure 4A, indicating that the mutation of fascin1 did not influence IFN-β production (Fig. 4F). Poly (I:C) strengthened the association of endogenous fascin1 and IKKε in DLD-1 cells, as shown in Figure 4G. This result suggests that fascin1 might act as an initial brake on RLR signaling that is released by stimulation but not as a negative feedback regulator, enabling the interaction to increase after stimulation. Binding site characterization was performed using HEK293T cells instead of DLD-1 cells, since the co-immunoprecipitation of fascin1/IKKε with overexpressed IKKε was less pronounced in the DLD-1 cell line. Since the mRNA levels of TBK1 and IKKε without poly (I:C) treatment were similar between the control and fascin1-deleted DLD-1 cells, fascin1 deletion was confirmed to have no effect on the level of RIG-I signaling molecules (Fig. 4H).

Poly (I:C) suppressed growth, migration and invasion in fascin1-deleted DLD-1 cells—Next, the anti-cancer effect of fascin1 knockdown on RIG-I signaling was investigated. The knockdown of fascin1 did not alter cell growth (Fig. 5A), as shown in Figure 1C, but growth in fascin1-deleted cells was markedly suppressed by poly (I:C) transfection, compared with PBS-only treatment. This finding was consistent with the augmented cell death (16%-22%) observed by poly (I:C) transfection in fascin1-deleted cells (Fig. 5B). Cell migration and invasion were inhibited by fascin1 knockdown (Fig. 5C), similar to the findings shown in Figure 1D, and were more strongly suppressed by poly (I:C) transfection, compared with PBS treatment, in fascin1-deleted cells (Fig. 5C). We clarified that the impaired migration ability induced in fascin1-deleted DLD-1 cells under poly (I:C) treatment was dependent on the RIG-I mediated signaling pathway by the knockdown of RIG-I using siRNA (Fig. 5D). These results suggest that fascin1 binding to IKKε prevents cancer cell growth, migration and invasion via RIG-I signaling.

Knockdown of fascin1 enhanced the phosphorylation of Ser-727 in STAT1 by IFN-β treatment – To clarify the effects of fascin1 on the IFN feedback loop, the phosphorylation of STAT1 was evaluated in DLD-1 cells. In response to IFN-β treatment, the phosphorylation of Tyr-701 in STAT1 was activated in fascin1-deleted cells using the same kinetics as those occurring in control cells. In contrast, the phosphorylation of Ser-727 in STAT1 was remarkably enhanced in fascin1-deleted cells (Fig. 6A). Although the phosphorylation of Ser-727 in STAT1 has been shown to require p38 MAPK activity (21) and to be regulated by CDK8 (22), neither of these were related to fascin1 (data not shown). These findings implied that fascin1 modulated the feedback loop of the IFN-β signaling pathway by suppressing STAT1 Ser-727 phosphorylation. Based on the above findings, the role of fascin1 in the virus-dependent RIG-I signaling pathway (Left) and its IFN feedback loop (Right) in DLD-1 colon cancer cells was schematically proposed in Figure 6B.

DISCUSSION

In addition to activating dendritic cells, viral infection has also been found to induce endogenous IFN-β in human cancer cells (23). Fascin1 is involved in immune responses such as cytokine production (24). The present study clearly demonstrated the involvement of fascin1 in the dsRNA-dependent RIG-I signaling pathway of DLD-1 colon cancer cells upon viral stimulation. Whereas TLRs are located on the cell surface or in endosomes, where they recognize viral RNA and DNA, RIG-I and MDA5 are cytosolic nucleic acid sensors that recognize viruses intracellularly (24). Here, DLD-1 cells with or without fascin1 did not display differential responses to extracellular poly (I:C) treatment as evaluated using the IFN-β mRNA level. However, the mRNA levels of RIG-I, MDA5 and IFN-β were significantly

increased by intracellular poly (I:C) transfection in fascin1-deleted cells, indicating that the knockdown of fascin1 enhanced IFN-β production via a RIG-I-dependent pathway, and not via TLR3-mediated responses in DLD-1 cells.

RIG-I and MDA5 interact with IPS-1 leading to the recruitment of TRAF3 (TNF receptor-associating factor 3), TBK1 and IKKε, causing the nuclear translocation of IRF-3, or leading to the activation of IKKγ, IKKα and IKKβ, resulting in the activation of NF-κβ (19, 24). We examined the pathways that fascin1 recognizes as its target (i.e., the IKKε/IRF-3 pathway and the IKKγ/IKKα/NF-κβ pathway) under poly (I:C) transfection. No alterations were observed in the activation of NF-κβ/p65 between DLD-1 cells with or without fascin1, although dimerization of IRF-3 was evident in fascin1-deleted cells. IRF-3 dimerization is associated with the activation and translocation of IRF-3 from the cytoplasm to the nucleus (25) to induce IFN-β. This confirmed the influence of fascin1 on the IKKε/IRF-3 pathway by poly (I:C) transfection in DLD-1 cells.

We next searched for fascin1 associations with RIG-I, IPS-1, TBK1, IKKε and IRF-3. We concluded that fascin1 interacted with IKKε, rather than with RIG-I, IPS-1, TBK1 or IRF-3, using a luciferase reporter assay and co-immunoprecipitation; however, the mechanism by which IKKε-induced IFN-ß induction is impaired by fascin1 is completely unknown. One study revealed that the activation of IKKε is rapid, transient, and precedes a more prolonged activation of TBK1 in immune cells (26). Even though IKKε and TBK1 are generally treated as a complex, TBK1 is reported to be predominantly responsible for IRF3 activation, and the involvement of IKKε in the relation between TBK1 and IRF-3 remains uncertain (27). Capturing the behavior of IKKε may be difficult. Thus, the mechanism by which fascin1 impairs the induction of IFN-ß by associating with IKKε is likely to be complex but needs to be resolved. IKKε influences cell proliferation and transformation and is thereby classified as an oncogene (28); meanwhile, the overexpression of IKKε has been documented to activate IRF-3 (29), which induces IFN-β production by viral infection. In our experiments, IKKε without an association with fascin1 was considered to promote the production of IRF-7, IFN-β, IFITs and IP-10 to suppress cell growth and invasion under poly (I:C) treatment. The diminished cell growth was accompanied by an increase in apoptosis. Regarding its inhibitory effect on growth, poly (I:C) has been reported to cause apoptosis resulting from ROS-mediated DNA damage and IFN-β-mediated growth arrest in renal cell carcinoma (30). However, the mechanism by which the knockdown of fascin1 enhances apoptosis remains unclear.

As for the inhibitory effect of fascin1 knockdown on cell invasion, we observed a significant increase in IRF-7 expression in fascin1-deleted cells. According to Li et al. (31), highly expressed miR-762 in breast cancer cell lines promoted cell invasion by down-regulating IRF-7. Furthermore, patients exhibiting a high expression of IRF-7-regulated genes in primary tumors were associated with prolonged bone metastasis-free survival, and the restoration of IRF-7 or the administration of IFN to breast cancer cells led to a reduction in bone metastases (32). Thus, the inhibitory effect of fascin1 knockdown on invasion in DLD-1 cells might be regarded as depending largely on an increase in IRF-7. Concerning INF-β and IP-10, the former inhibited the proliferation and invasion of pancreatic cancer cells (33) and the latter was involved in the induction of apoptosis and the inhibition of colorectal cancer growth (34). On the other hand, excreted endogenous type I IFN recruits and activates CD8α+ dendritic cell populations, resulting in tumor regression (35) as shown in Figure 6B. Therefore, the inhibition of IFN production is preferable for tumor cell survival, which may be, in part, mediated by fascin1.

Since IKKε directly phosphorylates STAT1 (36) and exerts antitumor activity (37,38), we investigated how fascin1 affects STAT1 phosphorylation in the IFN feedback loop. RIG-I facilitates the positive feedback

loop of type I IFN production (39). In this pathway, IFN-β stimulates the JAK-STAT pathway leading to the phosphorylation of STAT1 and STAT2 (40, 41). STAT1/2 heterodimers and IRF9 form a protein complex that participates in this feedback loop (42). In our experiments with DLD-1 cells, IFN-β increased the phosphorylation of Tyr-701 in STAT1, similar to the results of another report (43), although fascin1 knockdown did not affect the degree of phosphorylation. Perwitasari et al. (44) reported that IKKε phosphorylated Ser-708 in STAT1 by IFN-β treatment, while Zhang et al. (45) dismissed this possibility in T cells, suggesting that IKKε relayed signaling depending on the cell type and apical signal. This phosphorylation site of IKKε in IFN-β signaling is believed to exhibit diversity. In the current study, the phosphorylation of Ser-727 in STAT1 was enhanced in fascin1-deleted cells, indicating the possibility of the suppressive phosphorylation control of Ser-727 in STAT1 by fascin1. The association of fascin1 with IKKε is most likely involved in the phosphorylation of Ser-727 in the IFN-β feedback loop in DLD cells. Taken together, our results provide evidence that fascin1 not only participates in the initial IFN-β production stage but is also involved in the IFN signaling feedback loop by associating with IKKε, as proposed in Figure 6B. Identifying the roles of the fascin1/IKKε association on STAT1 in the feedback loop will be a major issue in future research. In conclusion, we have identified fascin1 as a suppressor of the RIG-I signaling pathway associated with IKKε in DLD-1 colon cancer cells, resulting in the suppression of immune responses to viral infection. Further study of the possible therapeutic application of fascin1 is warranted.

EXPERIMENTAL PROCEDURES

Cell culture—DLD-1, L929 and HEK293T cells were maintained in Dulbecco's modified Eagle's medium (Sigma-Aldrich, St. Louis, MO). All the cultures were supplemented with 10% heat-inactivated FBS and penicillin/streptomycin.

Antibodies and reagents—Antibodies against phospho-IRF-3 (Ser396), NF-κB/p65, phospho-NF-κB/p65 (S536), p38 MAPK, phosphor-p38 MAPK (Thr180/Tyr182), STAT1, phosphor-STAT-1 (Tyr701) and phosho-STAT1 (Ser727) were purchased from Cell Signaling Technology (Danvers, MA); antibodies against β-actin, fascin1 and IRF-3 were obtained from Santa Cruz Biotechnology (Dallas, TX); antibodies against DDDDK-tag and Myc-tag were procured from MBL (Nagoya, Japan); and secondary antibodies were obtained from Invitrogen (Carlsbad, CA). Annexin V alexa 647 (BioLegend, San Diego, CA), 7-aminoactinomycin D (7-AAD, Enzo Life Science, Farmingdale, NY), rhodamine phalloidin (Cytoskeleton, Inc., Denver, CO), poly (I:C) (Sigma-Aldrich and InvivoGen, San Diego, CA; used at a 5 μg/mL concentration), pSINsi-hU6 vector (TaKaRa Bio, Inc., Shiga, Japan), pRL-TK vector (Promega, Madison, WI), and pcDNA3 and pFLAG-CMV4 vectors (Invitrogen) were also used.

Retroviral transduction—The fascin1 knockdown vector was constructed using the pSINsi-hU6 shRNA expression retrovirus vector. We used two target sequences of human fascin1, as follows: 5'-GGTGGGCAAGGACGAGCTC-3' and 5'-GCCTGAAGAAGAAGCAGAT-3' (6). DLD-1 or L929 cells stably expressing fascin1-shRNA were selected in 500 μg/mL of G418-containing medium.

Knockdown of RIG-I using siRNA

The target sequences for the two pairs of human RIG-I gene were as follows:

Control

Sense 5'-UUCUCCGAACGUGUCAACGUTT-3'

Antisense 5'-ACGUGACACGUUCGGAGAATT-3'

RIG-I #1

Sense 5'-UAAGGUUGUUCACAAGAAUCUGUGG-3'

Antisense

5'-CCACAGAUUCUUGUGAACAACCUUA-3'

RIG-I #2

Sense 5'-UGGACAUGAAUUCUCACUAAGAUUC-3'

Antisense

5'-GAAUCUUAGUGAGAAUUCAUGUCCA-3'

DLD-1 cells were transfected with siRNAs (10 nM) using Lipofectamine RNAi MAX Reagent (Thermo Fisher Scientific Inc., Waltham, MA).

Immunofluorescence—Cells were fixed with 4% PFA in PBS and permeabilized with Triton X-100. After blocking, the cells were incubated with primary antibodies overnight at 4ºC, followed by incubation with secondary antibodies for 60 min. A confocal microscopy analysis was performed using a Leica TCS SP2 AOBS (Leica Microsystems, Wetzlar, Hessen, Germany).

Boyden-chamber cell migration assay—A total of 1×10^5 cells suspended in 500 μL of serum-free medium were plated onto the cell culture inserts (8-μm pore size; Becton Dickinson, Franklin Lakes, NJ), which were then placed into 24-well dishes containing 10% FBS-culture medium. Cells in the upper chamber were removed using a cotton swab 20-24 h later, and the migrated cells were fixed in 100% methanol and stained with crystal violet solution (0.2% crystal violet in 2% ethanol) for 10 min. Three randomly selected fields on the lower side of the inserts were photographed, and the migrated cells were counted.

Cell invasion assay—The cell invasion assays were identical to the cell migration assay apart from the pre-coating of the cell culture insert with 2 mg/mL of Matrigel™ matrix basement membrane (Becton Dickinson) for 4-5 h at 37ºC. The invasion period was 40-48 h.

Real-time RT-PCR—Total RNA was prepared using RNAiso plus (TaKaRa Bio, Inc.), and cDNA was synthesized using PrimeScript RT Master Mix (TaKaRa Bio, Inc.). A Thermal Cycler Dice™ Real-time system (TaKaRa Bio, Inc.) was used. All the data were normalized to the expression of GAPDH mRNA and were presented as the fold-increase relative to the control cells. The primer sets that were used are listed in Table 1.

TABLE 1.
Primers used for real-time RT-PCR

Gene	Sequence
hu GAPDH	
	Forward 5'-CACCACCAACTGCTTAGCACC-3'
	Reverse 5'-CAGTCTTCTGGGTGGCAGTGATG-3'
hu Fascin1	
	Forward 5'-CCAACGAGAGGAACGTGTCCA-3'
	Reverse 5'-GGAAGGTCTCCTGGTCGGTC-3'
hu IFN-β	
	Forward 5'-GATTCATCTAGCACTGGCTGG-3'
	Reverse 5'-CTTCAGGTAATGCAGAATCC-3'
hu RIG-I	
	Forward 5'-TGATAGCAACAGTCAAACACA-3'
	Reverse 5'-AATTTGTCGCTAATCCGTGA-3'
hu MDA5	
	Forward 5'-TATGAAACCAGAGGAGTATGC-3'
	Reverse 5'-GGTTATTCTTGTAATGCTTGGC-3'
hu IRF-7	
	Forward 5'-TGCCTCGGAACTGTGAC-3'
	Reverse 5'-CAGGTAGATGGTATAGCGTG-3'
hu IFIT1(ISG56)	
	Forward 5'-CGCTATAGAATGGAGTGTCCA-3'
	Reverse 5'-TTTCCTCCACACTTCAGCA-3'
hu IFIT2(ISG54)	
	Forward 5'-CTAAAGCACCTCAAAGGGCA-3'
	Reverse 5'-GCATAGTTTCCCCAGGTGAC-3'
hu IFIT3(ISG60)	
	Forward 5'-AGTCTAGTCACTTGGGGAAAC-3'
	Reverse 5'-ATAAATCTGAGCATCTGAGAGTC-3'
hu CXCL10 (IP-10)	
	Forward 5'-TGACTCTAAGTGGCATTCAAGGAG-3'
	Reverse
5'-TTTTTCTAAAGACCTTGGATTAACAGG-3'	
TBK1	
	Forward 5'-TGATAGCAACAGTCAAACACA -3'
	Reverse 5'- TAGAACTTGGATAAATTGGG -3'
IKKε	
	Forward 5'- ACTCTGGAAGTGGCAAGGACAT -3'
	Reverse 5'- TACCTGATCCCGGCTCTTCACCA -3'

Flow cytometric analysis—Apoptotic cells were analyzed by staining with Annexin V Alexa-647 and 7-AAD in Annexin V staining buffer (10 mM HEPES-KOH [pH7.4], 140 mM NaCl, 2.5 mM $CaCl_2$) using a BD FACSCanto II (Becton Dickinson) with Kaluza software (Beckman Coulter, Inc., Brea, CA).

Immunoblot analysis—Cells were washed with Hank's buffered salt solution and lysed with WCE buffer (20 mM Tris-HCl

[pH7.4], 150 mM NaCl, 0.5% sodium deoxycholate, 1% NP-40, 1% SDS, 2 mM EDTA, 1 mM PMSF, 250 μg/mL Na_3VO_4, 25 mM NaF, 1×protease inhibitor cocktail [Roche Diagnostics, Basel, Switzerland]), then sonicated on ice. Extracts were separated using SDS-PAGE.

Native-PAGE—Cells were lysed with Clear Native-PAGE cell lysis buffer (50 mM Tris-HCl [pH7.5], 150 mM NaCl, 1% NP-40, 1 mM PMSF, 5 mM Na_3VO_4, 1×complete protease inhibitor cocktail) for 45 min on ice and then centrifuged at 13,000 rpm for 10 min at 4ºC. The protein concentration was adjusted using the Quick Start Bradford Protein Assay kit (Bio-Rad Laboratories, Hercules, CA). Proteins were separated in the absence of SDS in 4-20% gradient gels (Mini-PROTEAN TGX Precast gel, Bio-Rad) using cathode buffer (25mM Tris, 192mM Glycine, 0.2% Sodium deoxycholate) and anode buffer (25mM Tris, 192mM Glycine). Proteins were transferred to PVDF membranes, which were probed with a 1:1000 dilution of anti-IRF-3 antibody. Goat anti-rabbit IgG-HRP at a 1:5000 dilution was used as the secondary antibody.

Luciferase reporter assay—HEK293T cells were seeded into 12-well culture plates and transfected with plasmids encoding the -125+19 mouse IFN-β luciferase reporter (firefly luciferase; 100 ng) and pRL-TK (renilla luciferase plasmid; 10 ng, Promega), together with 100 ng of pcDNA3 vector encoding RIG-I, IPS-1, TBK1, IKKε or IRF-3(5D) at increasing concentrations (0, 100, or 200 ng) of pFLAG-CMV4 with fascin1 using GeneJuice Transfection Reagent (Merck Millipore, Darmstadt, Germany). IRF-3(5D) is a variant of IRF3 in which Ser-396, Ser-398, Ser-402, Thr-404, and Ser-405 have been substituted with phospho-mimetic Asp to produce a constitutively active form (46). Empty pcDNA3 and pFLAG-CMV4 vectors were used to maintain equal amounts of DNA among the wells. The cells were lysed with 1×Glo cell lysis buffer (Promega) 24 h after transfection. Luciferase activity was measured using a Dual-Luciferase Assay (Promega) with a POWERSCAN4 plate reader (DS Pharma Biomedical Co., Ltd., Osaka, Japan) according to the manufacturer's protocol. The reporter gene activity was determined by normalization of the firefly luciferase activity to that of renilla luciferase.

Co-immunoprecipitation—TBK1, IKKε or IRF-3(5D) were inserted into pFLAG-CMV4 vectors, and fascin1 was inserted into the Myc-pcDNA3 vector for transient transfection into HEK293T cells. Lysates in NP-40 lysis buffer (50 mM Tris-HCl [pH7.4], 150 mM NaCl, 1 mM $MgCl_2$, 0.5% NP-40, 10 mM NaF, 1 mM Na_3VO_4, 1 mM PMSF, and 1×protease inhibitor cocktail) were incubated with the indicated antibodies for 1 h at 4ºC, followed by the addition of protein-G Sepharose beads (Roche) for an additional 2 h at 4ºC. After centrifugation, the beads were washed with NP-40 lysis buffer and then heated to 98ºC for 5 min in Laemmli sample buffer. Following a brief centrifugation, the supernatants were separated using SDS-PAGE.

Statistical analysis—The statistical significance of the results was calculated using the Student *t*-test or a one-way ANOVA followed by Tukey's and Dunnett's multiple comparison tests. Differences were considered significant at $P < 0.05$. All the data were presented as the mean ± standard deviation.

Acknowledgements: This work was funded by a grant for General Scientific Research (JP20012020 and JP26293300) from the Ministry of Education, Culture, Sports, Science and Technology of Japan. We thank Norie Araki at Tumor Genetics and Biology, Kumamoto University, for providing technical support.

Conflict of interest: The authors declare that they have no conflicts of interest with the contents of this article.

Author contributions: TM, SH, and ST conceived the study, performed the experiments and wrote the paper. MK designed and constructed the vectors for the expression of the shRNA and mutant proteins and analyzed the mutant phenotypes in bacteria. CF designed, performed and analyzed the experiments shown in Figure 3 (Native-PAGE). MT provided technical assistance and contributed to the preparation of the figures. AK and SM analyzed the experiments, coordinated the study, and finalized the paper. All the authors have reviewed the results and approved the final version of the manuscript.

REFERENCES

1. Adams, J.C. (1997) Characterization of cell-matrix adhesion requirements for the formation of fascin microspikes. *Mol. Biol. Cell.* **8**, 2345-2363
2. Adams, J.C. (2004) Roles of fascin in cell adhesion and motility. *Curr. Opin. Cell Biol.* **16**, 590-596
3. Snyder, M., Huang, J., Huang, X.Y., and Zhang, J.J. (2014) A signal transducer and activator of transcription 3·Nuclear Factor κB (Stat3·NFκB) complex is necessary for the expression of fascin in metastatic breast cancer cells in response to interleukin (IL)-6 and tumor necrosis factor (TNF)-α. *J. Biol. Chem.* **289**, 30082-30089
4. Hashimoto, Y., Parsons, M., and Adams, J.C. (2007) Dual actin-bundling and protein kinase C-binding activities of fascin regulate carcinoma cell migration downstream of Rac and contribute to metastasis. *Mol. Biol. Cell.* **18**, 4591-4602
5. Ma, Y., Faller, W.J., Sansom, O.J., Brown, E.R., Doig, T.N., Melton, D.W., and Machesky, L.M. (2015) Fascin expression is increased in metastatic lesions but does not correlate with progression nor outcome in melanoma. *Melanoma Res.* **25**, 169-172
6. Chen, L., Yang, S., Jakoncic, J., Zhang, J.J., and Huang, X.Y. (2010) Migrastatin analogues target fascin to block tumour metastasis. *Nature* **464**, 1062-1066
7. Huang, F.K., Han, S., Xing, B., Huang, J., Liu, B., Bordeleau, F., Reinhart-King, C.A., Zhang, J.J., and Huang, X.Y. (Jun 17, 2015) Targeted inhibition of fascin function blocks tumour invasion and metastatic colonization. *Nat. Commun.* 6:7465. doi: 10.1038/ncomms8465
8. Kim, J..K, Lee, S.M., Suk, K., and Lee, W.H. (2011) A novel pathway responsible for lipopolysaccharide-induced translational regulation of TNF-α and IL-6 expression involves protein kinase C and fascin. *J. Immunol.* **187**, 6327-6334
9. Besch, R., Poeck H, Hohenauer T, Senft D, Häcker G, Berking C, Hornung V, Endres S, Ruzicka T, Rothenfusser, S., and Hartmann, G. (2009) Proapoptotic signaling induced by RIG-I and MDA-5 results in type I interferon-independent apoptosis in human melanoma cells. *J. Clin. Invest.* **119**, 2399-2411
10. Jiang, L.J., Zhang, N.N., Ding, F., Li, X.Y., Chen, L., Zhang, H.X., Zhang, W., Chen, S.J., Wang, Z.G., Li, J.M., Chen, Z., and Zhu, J. (2011) RA-inducible gene-I induction augments STAT1 activation to inhibit leukemia cell proliferation. *Proc. Natl. Acad. Sci. USA.* **108**, 1897-1902
11. Palchetti, S., Starace, D., De Cesaris, P., Filippini, A., Ziparo, E., and Riccioli, A. (2015) Transfected poly(I:C) activates different dsRNA receptors, leading to apoptosis or immunoadjuvant response in androgen-independent prostate cancer cells. *J. Biol. Chem.* **290**, 5470-5483
12. Duewell, P., Steger, A., Lohr, H., Bourhis, H., Hoelz, H., Kirchleitner, S.V., Stieg, M.R., Grassmann, S., Kobold, S., Siveke, J.T., Endres, S., and Schnurr, M. (2014) RIG-I-like helicases induce immunogenic cell death of pancreatic cancer cells and sensitize tumors toward killing by CD8(+) T cells. *Cell Death Differ.* **21**, 1825-1837

13. Roulois, D., Loo Yau, H., Singhania, R., Wang, Y., Danesh, A., Shen, S.Y., Han, H., Liang, G., Jones, P.A., Pugh, T.J., O'Brien, C., De Carvalho, and D.D. (2015) DNA-Demethylating Agents Target Colorectal Cancer Cells by Inducing Viral Mimicry by Endogenous Transcripts. *Cell* **162**, 961-973
14. Morosky, S.A., Zhu, J., Mukherjee, A., Sarkar, S.N., and Coyne, C.B. (2011) Retinoic acid-induced gene-I (RIG-I) associates with nucleotide-binding oligomerization domain-2 (NOD2) to negatively regulate inflammatory signaling. *J. Biol. Chem.* **286**, 28574-28583
15. Mukherjee, A., Morosky, S.A., Shen, L., Weber, C.R., Turner, J.R., Kim, K.S., Wang, T., and Coyne, C.B. (2009) Retinoic acid-induced gene-1 (RIG-I) associates with the actin cytoskeleton via caspase activation and recruitment domain-dependent interactions. *J. Biol. Chem.* **284**, 6486-6494
16. Vignjevic, D., Kojima, S., Aratyn, Y., Danciu, O., Svitkina, T., and Borisy, G.G. (2006) Role of fascin in filopodial protrusion. *J. Cell. Biol.* **174**, 863-875
17. Yamakita, Y., Matsumura, F., and Yamashiro, S. (2009) Fascin1 is dispensable for mouse development but is favorable for neonatal survival. *Cell Motil. Cytoskeleton* **66**, 524-534
18. Sadik, C.D., Bachmann, M., Pfeilschifter, J., and Mühl, H. (2009) Activation of interferon regulatory factor-3 via toll-like receptor 3 and immunomodulatory functions detected in A549 lung epithelial cells exposed to misplaced U1-snRNA. Nucleic Acids Res. 37, 5041-5056
19. Seth, R.B., Sun, L., Ea, C.K., and Chen, Z.J. (2005) Identification and characterization of MAVS, a mitochondrial antiviral signaling protein that activates NF-kappaB and IRF-3. *Cell* **122**, 669-682
20. Ikeda, F., Hecker, C.M., Rozenknop, A., Nordmeier, R.D., Rogov, V., Hofmann, K., Akira, S., Dötsch, V., and Dikic, I. (2007) Involvement of the ubiquitin-like domain of TBK1/IKK-i kinases in regulation of IFN-inducible genes. *EMBO J.* **26**, 3451-3462
21. Sadzak, I., Schiff, M., Gattermeier, I., Glinitzer, R., Sauer, I., Saalmüller, A., Yang, E., Schaljo, B., and Kovarik, P. (2008) Recruitment of Stat1 to chromatin is required for interferon-induced serine phosphorylation of Stat1 transactivation domain. *Proc. Natl. Acad. Sci. USA*. **105**, 8944-8949
22. Bancerek, J., Poss, Z.C., Steinparzer, I., Sedlyarov, V., Pfaffenwimmer, T., Mikulic, I., Dölken, L., Strobl, B., Müller, M., Taatjes, D.J., and Kovarik, P. (2013) CDK8 kinase phosphorylates transcription factor STAT1 to selectively regulate the interferon response. *Immunity* **38,** 250-262
23. Gatti, G., Nuñez, N.G., Nocera, D.A., Dejager, L., Libert, C., Giraudo, C., and Maccioni, M. (2013) Direct effect of dsRNA mimetics on cancer cells induces endogenous IFN-β production capable of improving dendritic cell function. *Eur. J. Immunol.* **43**, 1849-1861
24. Diamond, M.S., and Farzan, M. (2013) The broad-spectrum antiviral functions of IFIT and IFITM proteins. *Nat. Rev. Immunol.* **13**, 46-57
25. Yoneyama, M., Suhara, W., Fukuhara, Y., Fukuda, M., Nishida, E., and Fujita, T. (1998) Direct triggering of the type I interferon system by virus infection: activation of a transcription factor complex containing IRF-3 and CBP/p300. *EMBO J.* **17**, 1087-1095

26. Clark, K., Takeuchi, O., Akira. S., and Cohen, P. (2011) The TRAF-associated protein TANK facilitates cross-talk within the IkappaB kinase family during Toll-like receptor signaling. *Proc Natl Acad Sci U S A*. **108**, 17093-17098
27. Guo, B., and Cheng, G. (2007) Modulation of the interferon antiviral response by the TBK1/IKKi adaptor protein TANK. *J. Biol. Chem.* **282**, 11817-11826
28. Verhelst, K., Verstrepen, L., Carpentier, I., and Beyaert, R.**.** **(**2013) IκB kinase ε (IKKε): a therapeutic target in inflammation and cancer. *Biochem. Pharmacol.* **85**, 873-880
29. Koop, A., Lepenies, I., Braum, O., Davarnia, P., Scherer, G., Fickenscher, H., Kabelitz, D., and Adam-Klages, S. (2011) Novel splice variants of human IKKε negatively regulate IKKε-induced IRF-3 and NF-kB activation. *Eur. J. Immunol.* **41**, 224-234
30. Harashima, N., Minami, T., Uemura, H., and Harada, M. (Sep 17, 2014) Transfection of poly(I:C) can induce reactive oxygen species-triggered apoptosis and interferon-β-mediated growth arrest in human renal cell carcinoma cells via innate adjuvant receptors and the 2-5A system. *Mol. Cancer* 13:217. doi: 10.1186/1476-4598-13-217
31. Li, Y., Huang, R., Wang, L., Hao, J., Zhang, Q., Ling, R., and Yun, J. (2015) microRNA-762 promotes breast cancer cell proliferation and invasion by targeting IRF-7 expression. *Cell Prolif.* **48**, 643-649
32. Bidwell, B.N., Slaney, C.Y., Withana, N.P., Forster, S., Cao, Y., Loi, S., Andrews, D., Mikeska, T., Mangan, N.E., Samarajiwa, S.A., de Weerd, N.A., Gould, J., Argani, P., Möller, A., Smyth, M.J., Anderson, R.L., Hertzog, P.J., and Parker, B.S. (2012) Silencing of IRF-7 pathways in breast cancer cells promotes bone metastasis through immune escape. *Nat. Med.* **18**, 1224-1231
33. Booy, S., van Eijck, C.H., Janssen, J.A., Dogan, F., van Koetsveld, P.M., and Hofland, L.J. (2015) IFN-β is a potent inhibitor of insulin and insulin like growth factor stimulated proliferation and migration in human pancreatic cancer cells. *Am. J. Cancer Res.* **5**, 2035-2046
34. Liu, M., Guo, S., and Stiles, J.K. (2011) The emerging role of CXCL10 in cancer (Review). Oncol. Lett. **2**, 583-589
35. Diamond, M.S., Kinder, M., Matsushita, H., Mashayekhi, M., Dunn, G.P., Archambault, J.M., Lee, H., Arthur, C.D., White, J.M., Kalinke, U., Murphy, K.M., and Schreiber, R.D. (2011) Type I interferon is selectively required by dendritic cells for immune rejection of tumors. *J. Exp. Med.* **208**, 1989–2003
36. Tenoever, B.R., Ng, S.L., Chua, M.A., McWhirter, S.M., García-Sastre, A., and Maniatis, T. (2007) Multiple functions of the IKK-related kinase IKKepsilon in interferon-mediated antiviral immunity. *Science* **315**, 1274-1278
37. Clément, J.F., Meloche, S., and Servant, M.J. (2008) The IKK-related kinases: from innate immunity to oncogenesis. *Cell Res.* **18**, 889-899
38. Chen, J., Zhao, J., Chen, L., Dong, N., Ying, Z., Cai, Z., Ji, D., Zhang, Y., Dong, L., Li, Y., Jiang, L., Holtzman, M.J., and Chen, C. (Sep 8, 2015) STAT1 modification improves therapeutic effects of interferons on lung cancer cells. *J. Transl. Med.* 13:293. doi: 10.1186/s12967-015-0656-0
39. Kim, M.J., Hwang, S.Y., Imaizumi, T., and Yoo, J.Y. (2008) Negative feedback regulation of RIG-I-mediated antiviral signaling by interferon-induced ISG15 conjugation. *J. Virol.* **82**,

1474-1483
40. Hengel, H., Koszinowski, U.H., and Conzelmann, K.K. (2005) Viruses know it all: new insights into IFN networks. *Trends Immunol.* **26**, 396-401
41. Stark, G.R., Kerr, I.M., Williams, B.R., Silverman, R.H., and Schreiber, R.D. (1998) How cells respond to interferons. *Annu. Rev. Biochem.* **67,** 227-264
42. Zhao, H., Boije, H., Granberg, F., Pettersson, U., and Svensson, C. (2009) Activation of the interferon-induced STAT pathway during an adenovirus type 12 infection. *Virology* **392**, 186-195
43. Trilling, M., Le, V.T., Rashidi-Alavijeh, J., Katschinski, B., Scheller, J., Rose-John, S., Androsiac, G.E., Jonjic, S., Poli, V., Pfeffer, K., and Hengel, H. (2014) "Activated" STAT proteins: a paradoxical consequence of inhibited JAK-STAT signaling in cytomegalovirus-infected cells. *J. Immunol.* 192, 447-458
44. Perwitasari, O., Cho, H., Diamond, M.S., and Gale, M. Jr. (2011) Inhibitor of κB kinase epsilon (IKK(epsilon)), STAT1, and IFIT2 proteins define novel innate immune effector pathway against West Nile virus infection. *J. Biol. Chem.* **286**, 44412-44423
45. Zhang, J., Feng, H., Zhao, J., Feldman, E.R., Chen, S.Y., Yuan, W., Huang, C., Akbari, O., Tibbetts, S.A., and Feng, P. (2016) IκB Kinase ε is an NFATc1 kinase that inhibits T cell immune response. *Cell Rep.* **16**, 405-418 Chen L 1062-2
46. Lin, R., Heylbroeck, C., Pitha, P.M., and Hiscott, J. (1998) Virus-dependent phosphorylation of the IRF-3 transcription factor regulates nuclear translocation, transactivation potential, and proteasome-mediated degradation. *Mol. Cell. Biol.* **18**, 2986-2996

FIGURE LEGENDS

FIGURE 1. **Knockdown of fascin1 suppressed migration and invasion but not cell growth.** *A,* Stable knockdown of fascin1 in DLD-1 and L929 cells was confirmed using real-time RT-PCR ($n = 2$) and an immunoblot analysis. *B,* F-actin was stained with rhodamine-phalloidin, and images of filopodia in L929 cells were obtained using confocal microscopy. Original magnification, ×2560. *C,* Cell growth was measured using the MTS assay 48 h after the inoculation of DLD-1 cells ($n = 3$). *D,* Cell migration (n = 3) and invasion (n = 3) of DLD-1 cells were examined using the Boyden-chamber assay. (*$P < 0.05$, ***$P < 0.001$)

FIGURE 2. **Knockdown of fascin1 enhanced RIG-I/MDA5-mediated gene induction by the poly (I:C) transfection of DLD-1 and L929 cells.** *A,* Poly (I:C) was applied extracellularly for 6 h, and the mRNA expression of IFN-β was measured using real-time RT-PCR. *B-C, (B)* Poly (I:C) was transfected intracellularly for 6 h, and the mRNA expressions of IFN-β and IP-10, as well as those for (*C)* RIG-I, MDA5, IRF-7, and IFIT1s, were measured using real-time RT-PCR ($n = 6$). *D,* The re-expression of fascin1 using p-FLAG-CMV4 vector in fascin1-deleted cells was confirmed using real-time RT-PCR (n = 2). The alteration of IFN-ß mRNA expression by knockdown and the re-expression of fascin1 under poly (I:C) were examined using real-time RT-PCR (n = 3). (*$P < 0.05$, **$P < 0.01$)

FIGURE 3. **Knockdown of fascin1 enhanced poly (I:C)-induced IRF-3 activation in DLD-1 cells.** *A,* The phosphorylation of IRF-3 was examined using an immunoblot analysis. *B*, IRF-3 dimerization was detected using native-PAGE. The expressions of IRF-3 and fascin1 in whole cell lysates were examined using an immunoblot analysis. *C,* The phosphorylation of the NF-κB subunits p65/RelA in whole cell extracts was analyzed using an immunoblot analysis. WCL: whole cell lysates. Representative of 3 independent experiments

FIGURE 4. **Targets associated with fascin1 were analyzed using HEK293T cells.** *A,* Targets of fascin1 were evaluated using IFN-β luciferase reporter assays (n = 3). *B-C,* Targets of fascin1 were confirmed using *(B)* a co-immunoprecipitation analysis and *(C)* a reciprocal co-immunoprecipitation analysis. Data are representative of 3 independent experiments. *D,* Construction of full-length IKKε (complete) and its deletion mutants. The essential domain of IKKε required for its association with fascin1 was detected using a co-immunoprecipitation analysis. Data are representative of 3 independent experiments. *E,* Domains of fascin1 required for its association with IKKε were examined using a co-immunoprecipitation analysis. Data are representative of 2 independent experiments. *F,* IFN-β suppressive activity of three fascin1 mutants were evaluated using luciferase reporter assays (n = 3). *G*, Co-immunoprecipitation of endogenous fascin1 and IKKε in DLD-1 cells with or without poly (I:C). *H,* Influence of fascin1 knockout on mRNA level of TBK1 and IKKε in DLD-1 cells (n = 3). (**P* < 0.05, ***P* < 0.01, ****P* < 0.001)

FIGURE 5. **Transfection of poly (I:C) into fascin1-deleted DLD-1 cells suppressed cell growth, migration and invasion.** *A-B,* Forty-eight hours after poly (I:C) transfection, *(A)* cell growth was measured using the MTS assay (*n* = 6) and *(B)* apoptosis was determined using FACS 24 h later. *C,* Cell migration (*n* = 3) and invasion (*n* = 3) were examined using the Boyden chamber assay. *D,* Knockdown of RIG-I was confirmed using real-time RT-PCR (n = 2), and cell migration was compared between si-control and si-RIG-I-treated fascin1-deleted cells with or without poly (I:C) transfection (n = 3). (**P* < 0.05, ***P* < 0.01, ****P* < 0.001)

FIGURE 6. **Knockdown of fascin1 enhanced STAT1 Ser-727 phosphorylation in the IFN-β feedback loop in DLD-1 cells.** *A,* The phosphorylation of Tyr-701 and Ser-727 in STAT1 was analyzed using an immunoblot analysis after stimulation with 1 ng/mL of IFN-β for the indicated times. Data are representative of 2 independent experiments. *B,* Proposed schematic of fascin1 function in poly (I:C)-dependent RIG-I signaling (Left) and the IFN feedback loop (Right).

Fig.1

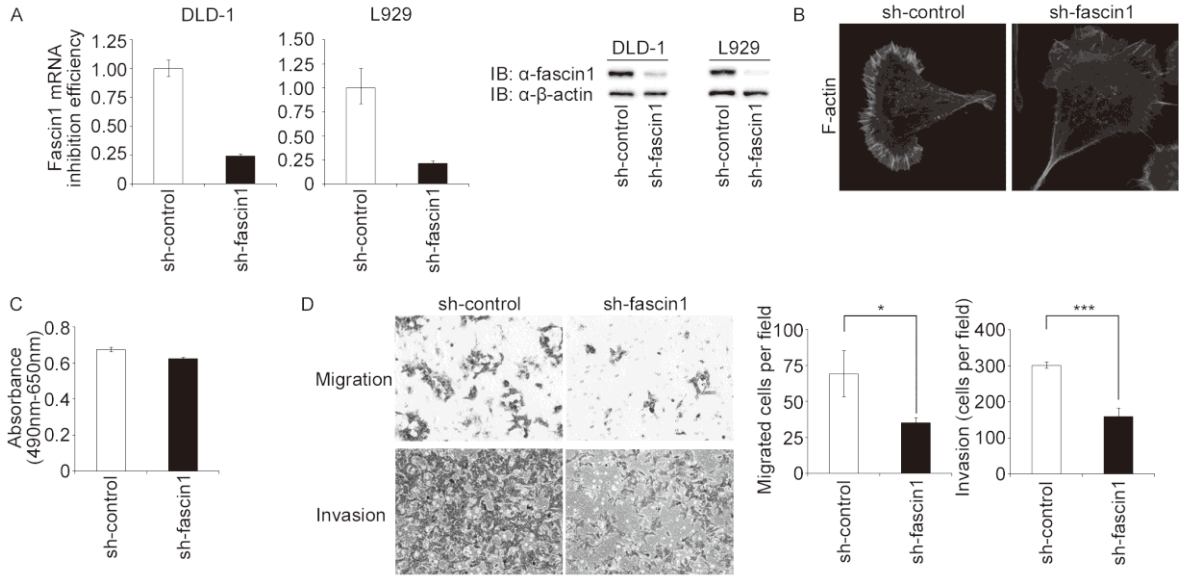
A
DLD-1
L929
Fascin1 mRNA inhibition efficiency
1.25
1.00
0.75
0.50
0.25
0
1.50
1.25
1.00
0.75
0.50
0.25
0
sh-control
sh-fascin1
sh-control
sh-fascin1
DLD-1
L929
IB: α-fascin1
IB: α-β-actin
sh-control
sh-fascin1
sh-control
sh-fascin1
B
sh-control
sh-fascin1
F-actin
C
Absorbance (490nm-650nm)
0.8
0.6
0.4
0.2
0
sh-control
sh-fascin1
D
sh-control
sh-fascin1
Migration
Invasion
Migrated cells per field
100
75
50
25
0
*
sh-control
sh-fascin1
Invasion (cells per field)
400
300
200
100
0
***
sh-control
sh-fascin1

Fig.2

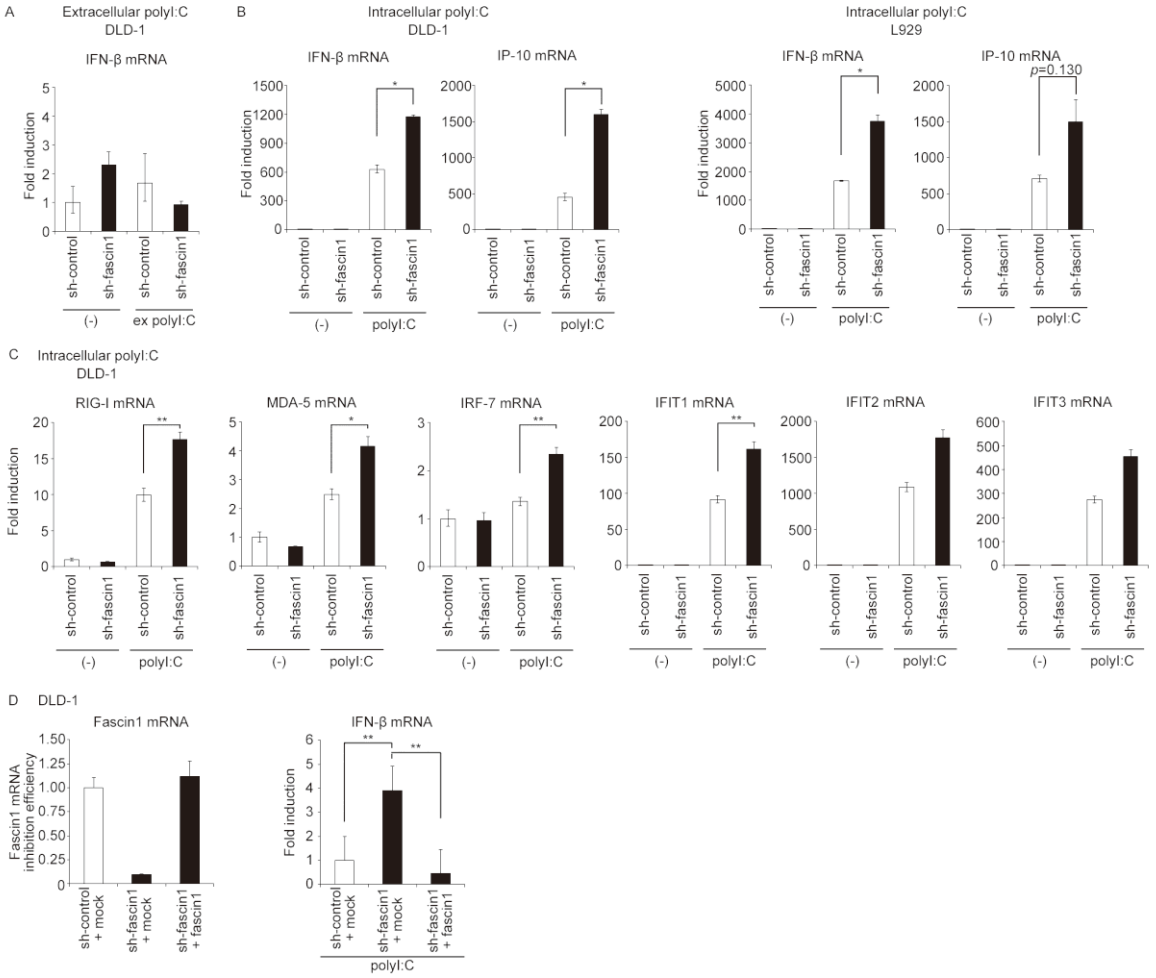
A
Extracellular polyI:C
DLD-1
IFN-β mRNA
Fold induction
sh-control
sh-fascin1
(-)
ex polyI:C
B
Intracellular polyI:C
DLD-1
IFN-β mRNA
IP-10 mRNA
polyI:C
Intracellular polyI:C
L929
p=0.130
C
Intracellular polyI:C
DLD-1
RIG-I mRNA
MDA-5 mRNA
IRF-7 mRNA
IFIT1 mRNA
IFIT2 mRNA
IFIT3 mRNA
D
DLD-1
Fascin1 mRNA
Fascin1 mRNA inhibition efficiency
sh-control + mock
sh-fascin1 + mock
sh-fascin1 + fascin1
IFN-β mRNA

Fig.3

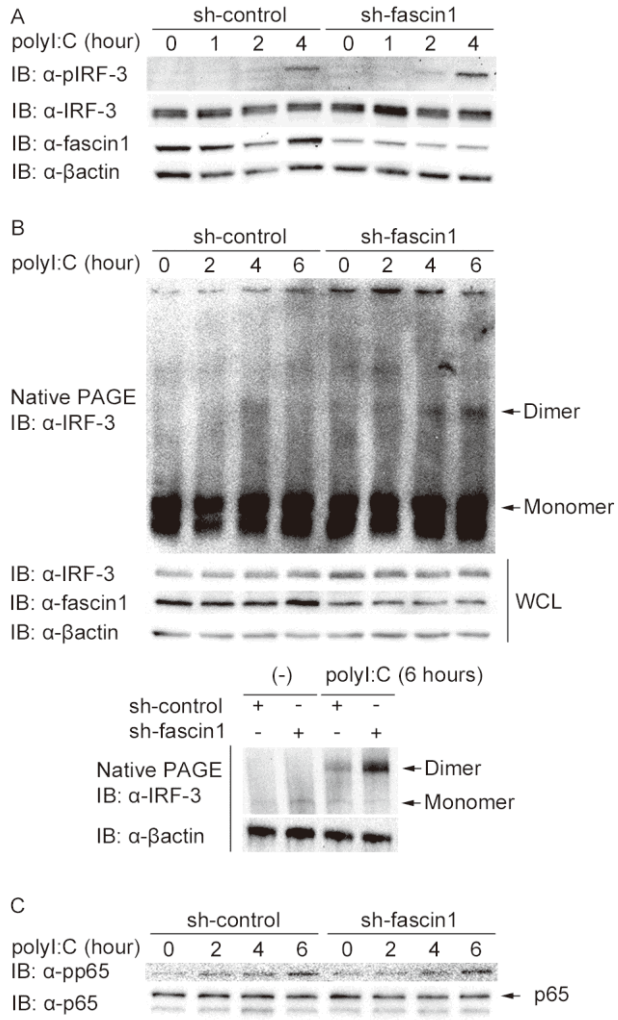
A
sh-control
sh-fascin1
polyI:C (hour)
0 1 2 4 0 1 2 4
IB: α-pIRF-3
IB: α-IRF-3
IB: α-fascin1
IB: α-βactin
B
sh-control
sh-fascin1
polyI:C (hour)
0 2 4 6 0 2 4 6
Native PAGE
IB: α-IRF-3
Dimer
Monomer
IB: α-IRF-3
IB: α-fascin1
IB: α-βactin
WCL
(-)
polyI:C (6 hours)
sh-control + - + -
sh-fascin1 - + - +
Native PAGE
IB: α-IRF-3
Dimer
Monomer
IB: α-βactin
C
sh-control
sh-fascin1
polyI:C (hour)
0 2 4 6 0 2 4 6
IB: α-pp65
IB: α-p65
p65

Fig.4 A-C

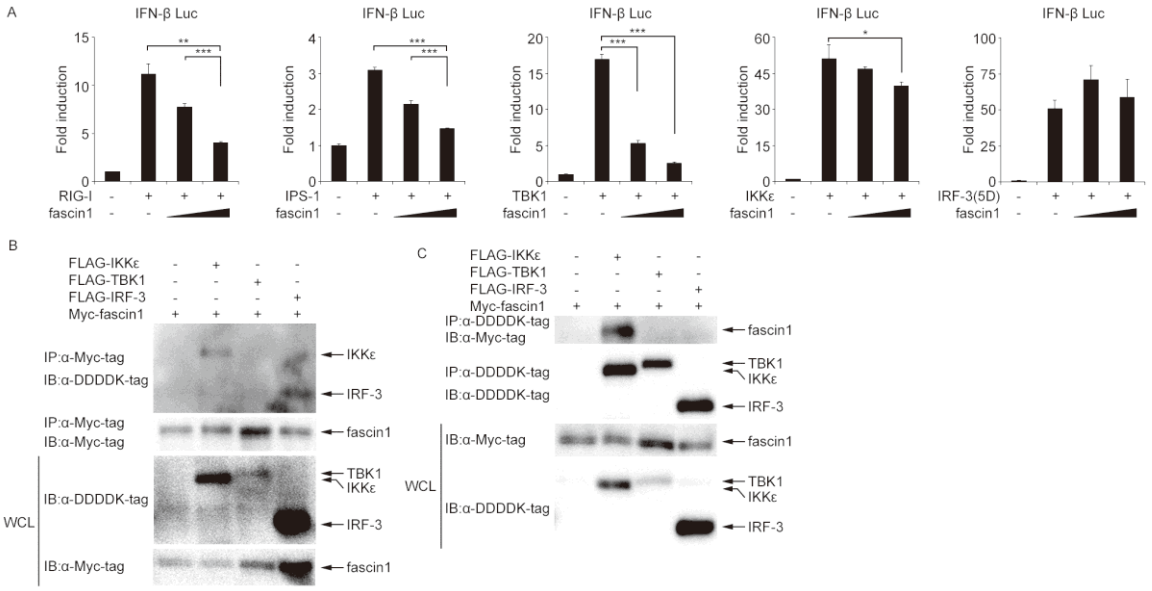
A
IFN-β Luc
Fold induction
RIG-I
IPS-1
TBK1
IKKε
IRF-3(5D)
fascin1
B
FLAG-IKKε
FLAG-TBK1
FLAG-IRF-3
Myc-fascin1
IP:α-Myc-tag
IB:α-DDDDK-tag
IB:α-Myc-tag
WCL
IKKε
IRF-3
fascin1
TBK1
C
IP:α-DDDDK-tag

Fig.4 D-H

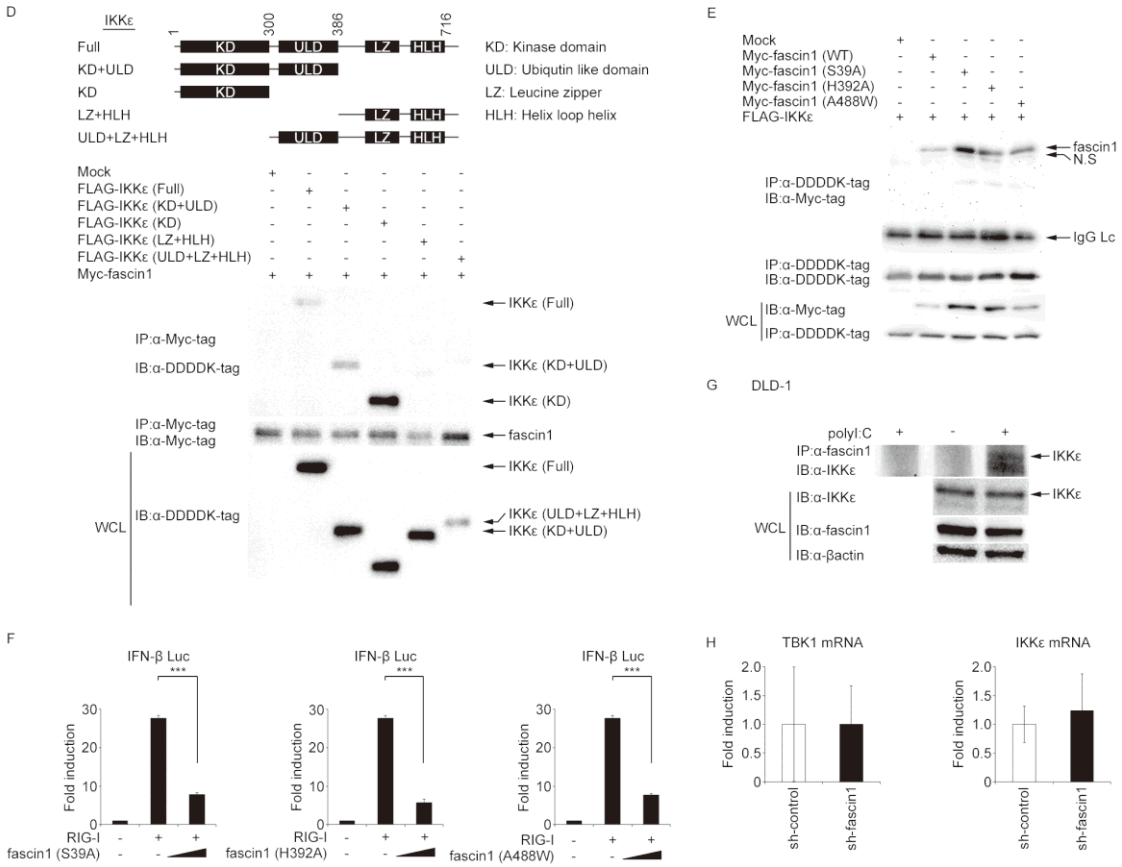
D
IKKε
1
300
386
716
Full
KD
ULD
LZ
HLH
KD+ULD
KD
LZ+HLH
ULD+LZ+HLH
KD: Kinase domain
ULD: Ubiqutin like domain
LZ: Leucine zipper
HLH: Helix loop helix
Mock
FLAG-IKKε (Full)
FLAG-IKKε (KD+ULD)
FLAG-IKKε (KD)
FLAG-IKKε (LZ+HLH)
FLAG-IKKε (ULD+LZ+HLH)
Myc-fascin1
IP:α-Myc-tag
IB:α-DDDDK-tag
IP:α-Myc-tag
IB:α-Myc-tag
WCL
IB:α-DDDDK-tag
IKKε (Full)
IKKε (KD+ULD)
IKKε (KD)
fascin1
IKKε (Full)
IKKε (ULD+LZ+HLH)
IKKε (KD+ULD)
E
Mock
Myc-fascin1 (WT)
Myc-fascin1 (S39A)
Myc-fascin1 (H392A)
Myc-fascin1 (A488W)
FLAG-IKKε
fascin1
N.S
IP:α-DDDDK-tag
IB:α-Myc-tag
IgG Lc
IP:α-DDDDK-tag
IB:α-DDDDK-tag
WCL
IB:α-Myc-tag
IP:α-DDDDK-tag
G
DLD-1
polyI:C
IP:α-fascin1
IB:α-IKKε
IKKε
WCL
IB:α-IKKε
IKKε
IB:α-fascin1
IB:α-βactin
F
IFN-β Luc
***
Fold induction
RIG-I
fascin1 (S39A)
fascin1 (H392A)
fascin1 (A488W)
H
TBK1 mRNA
IKKε mRNA
Fold induction
sh-control
sh-fascin1

Fig.5

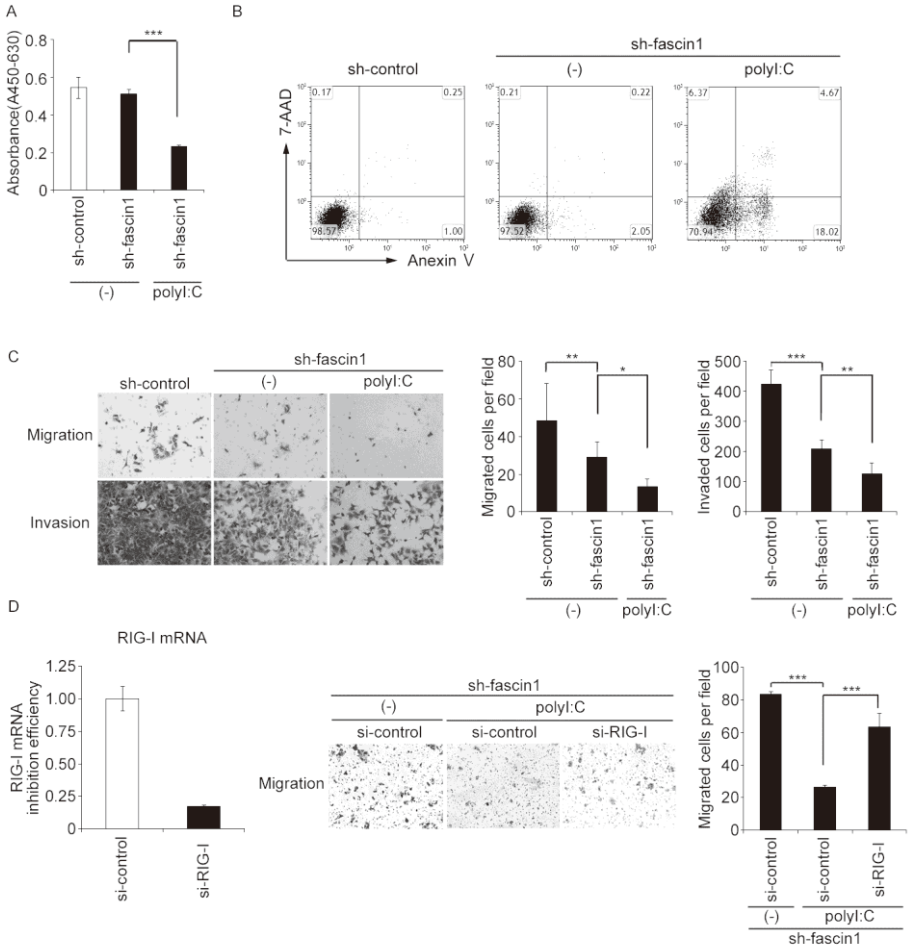
A
Absorbance(A450-630)
0.8
0.6
0.4
0.2
0
***
sh-control
sh-fascin1
sh-fascin1
(-)
polyI:C
B
sh-fascin1
sh-control
(-)
polyI:C
7-AAD
Anexin V
0.17
0.25
98.57
1.00
0.21
0.22
97.52
2.05
6.37
4.67
70.94
18.02
C
sh-fascin1
sh-control
(-)
polyI:C
Migration
Invasion
Migrated cells per field
80
60
40
20
0
**
*
Invaded cells per field
500
400
300
200
100
0
***
**
sh-control
sh-fascin1
sh-fascin1
(-)
polyI:C
D
RIG-I mRNA
RIG-I mRNA inhibition efficiency
1.25
1.00
0.75
0.50
0.25
0
si-control
si-RIG-I
sh-fascin1
(-)
polyI:C
si-control
si-control
si-RIG-I
Migration
Migrated cells per field
100
80
60
40
20
0
***
***
si-control
si-control
si-RIG-I
(-)
polyI:C
sh-fascin1

Fig.6

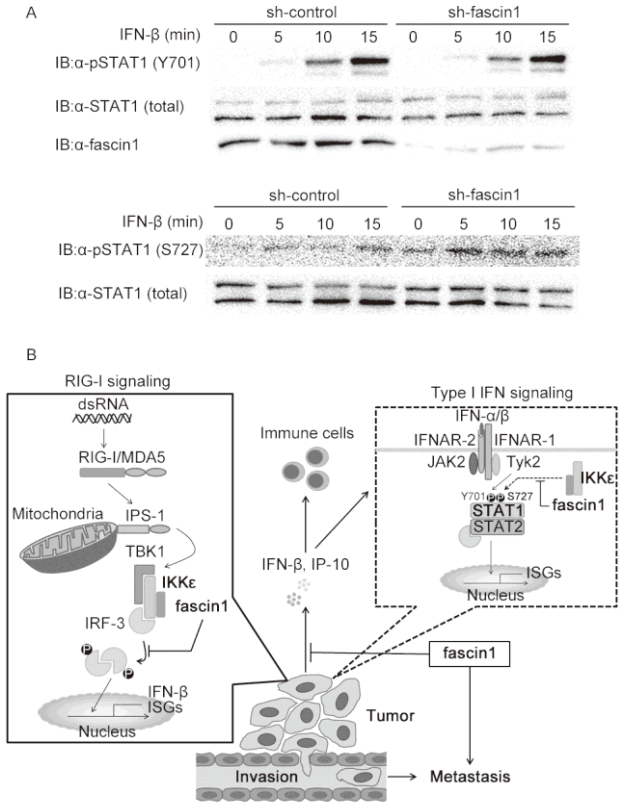
A
sh-control
sh-fascin1
IFN-β (min)
0 5 10 15 0 5 10 15
IB:α-pSTAT1 (Y701)
IB:α-STAT1 (total)
IB:α-fascin1
sh-control
sh-fascin1
IFN-β (min)
0 5 10 15 0 5 10 15
IB:α-pSTAT1 (S727)
IB:α-STAT1 (total)
B
RIG-I signaling
dsRNA
RIG-I/MDA5
Mitochondria
IPS-1
TBK1
IKKε
fascin1
IRF-3
P
P
IFN-β
ISGs
Nucleus
Immune cells
IFN-β, IP-10
Type I IFN signaling
IFN-α/β
IFNAR-2
IFNAR-1
JAK2
Tyk2
IKKε
Y701
P
S727
fascin1
STAT1
STAT2
ISGs
Nucleus
fascin1
Tumor
Invasion
Metastasis